Received: 27 January 2020 | Revised: 8 March 2020 | Accepted: 26 March 2020

DOI: 10.1002/jbt.22512

RESEARCH ARTICLE

WILEY

Synthesis, structural, cytotoxic and pharmacokinetic evaluation of some thiosemicarbazone derivatives

Mediha Süleymanoğlu[1] | Serap Erdem-Kuruca[2] | Tülay Bal-Demirci[3] | Namık Özdemir[4] | Bahri Ülküseven[3] | İlhan Yaylım[5]

[1]Department of Medical Biology, Istanbul Faculty of Medicine, Istanbul University, Çapa, Istanbul, Turkey

[2]Department of Physiology, Istanbul Faculty of Medicine, Istanbul University, Çapa, Istanbul, Turkey

[3]Department of Chemistry, Engineering Faculty, Istanbul University-Cerrahpasa, Avcilar, Istanbul, Turkey

[4]Department of Mathematics and Science Education, Faculty of Education, Ondokuz Mayıs University, Samsun, Turkey

[5]Department of Molecular Medicine, Aziz Sancar Institute of Experimental Medicine, Istanbul University, Çapa, Istanbul, Turkey

Correspondence
Mediha Süleymanoğlu, Department of Medical Biology, Istanbul Faculty of Medicine, Graduate School of Health Sciences, Istanbul University, Çapa, 34390, Istanbul, Turkey.
Email: mediha.suleymanoglu@istanbul.edu.tr

Funding information
Bilimsel Arastirma Projeleri Birimi, Istanbul Üniversitesi, Grant/Award Number: 49111; TÜBİTAK-SBAG, Grant/Award Number: 109S188; Ondokuz Mayis University, Grant/Award Number: PYO.FEN.1906.19.001

Abstract

Iron(III) and nickel(II) complexes bearing a thiosemicarbazone framework were synthesized by a one-pot synthesis method. The structures were characterized by elemental analysis, IR, ^{1}H NMR, APCI Mass, conductivity, magnetic moment measurements. Molecular and crystal structures of the iron(III) complex were obtained from single-crystal X-ray diffraction. The findings showed that the metal atom adopts a slightly distorted square-pyramidal coordination, with the four donor atoms of the thiosemicarbazone ligand defining the basal plane and a chloride atom occupying the apical position. In the crystal lattice, the structure is stabilized by intermolecular O—H···O and C—H···O interactions. The cytotoxic activity was studied by MTT assay, the expression levels of cytochrome P450 (CYP) enzymes by Western blot, and the lipophilicity (LogP) by using the shake-flask method, another pharmacokinetic parameter. The findings showed that the IC_{50} values decreased with the decrease of the LogP values of the substances. Cytochrome P450 expression levels were found specific for each compound and each cell line. As a result, the pharmacokinetic properties of the newly synthesized thiosemicarbazone compounds are crucial for oral administration and provide us with clues for prospective in vivo studies.

KEYWORDS

Cytochrome P450 (CYP) enzymes, cytotoxicity, lipophilicity, pharmacokinetics, thiosemicarbazones

1 | INTRODUCTION

Thiosemicarbazones have a framework C = N-N = C(SH)-NH_2 including more than one donor atom. These atoms can easily connect to a metal atom and/or a biomolecule such as DNA chemically or physically.[1–7] Thiosemicarbazones and their metal complexes are potential therapeutics for bacterial and viral infections [8–10] and show therapeutic activity against tuberculosis, leprosy,[11,12] malaria[13] and cancer.[4,14] Therefore, thiosemicarbazones and their metal complexes have attracted the attention of many researchers from different scientific fields. In particular, two compounds, COTI-2[15,16] and triapine[17–19] have recently come to the fore with further applications in the treatment of tuberculosis and in phase I and II clinical trials as a potent antitumor agent. Moreover, many substances and much research has been patented due to their strong potential in biological activities and their number is increasing day by day.

The pharmacokinetics of the newly synthesized thiosemicarbazone derivatives determines their potentials to be used as an anticancer drug.

The pharmacokinetics investigates whether the drugs are effective in the organism, by examining parameters such as absorption, distribution, metabolism, excretion, and toxicity (ADMET). One of the factors affecting the absorption of the drug is lipophilicity. Lipophilicity is a measure of the tendency of the cell membrane of the drug

to dissolve in a lipid bilayer.[20] Another pharmacokinetic property is biotransformation of the drugs. The most important drug-metabolizing enzymes are cytochrome P450s. CYP enzymes involved in xenobiotic metabolism are found mainly in the endoplasmic reticulum of hepatocytes, and, less commonly, in the small intestine, lung, kidney, and brain. The eight CYP members constitute 95% of CYPs. These are CYP3A4, CYP2D6, CYP2C9, CYP2E1, CYP2C19, CYP1A2, CYP2A6, and CYP2B6.[21] A majority of the commercial drugs are metabolized by CYP1A2, 2C9, 2D6, 2E1, and 3A4 CYP isoenzymes.[22] Also, MDR-1 (P-glycoprotein; P-gp), an ABCB1 gene product that limits the bioavailability of orally administered drugs, is an ATP dependent transporter involved in drug excretion. CYP3A4 and MDR-1 are synthesized by the same enterocytes. Therefore, the combined activity of these two proteins is important to understand drug pharmacokinetics.[23] Furthermore, the multiple drug resistance proteins MRP-1 and MRP-2 reduce the intracellular drug concentration by pumping out the drug.[24]

The present study was undertaken to determine the pharmacokinetics and cytotoxic properties of Fe(III) and Ni(II) complexes of thiosemicarbazones (Figure 1). These four new compounds were patented by the European Patent Office and the Turkish Patent Agency.[25,26] This study aims to synthesize Fe(III) and Ni(II) complexes and to investigate the cytotoxicity by MTT assay, the lipophilicity by the shake-flask method and the biotransformation profile by Western blot immunoassay. We also report here the molecular and crystal structures of the Fe(III) complex.

2 | MATERIALS AND METHODS

2.1 | Synthesis

2.1.1 | Chemicals and apparatus

All chemicals were of reagent grade and used as commercially purchased without further purification. The elemental analyses were determined on a Thermo Finnigan Flash EA 1112 Series Elemantar Analyzer and Varian Spectra-220/FS Atomic Absorption spectrometer. IR spectra of the compounds were recorded on a Cary 630 FTIR spectrometer with Diamond ATR from Agilent. The ^{1}H Nuclear Magnetic Resonance spectrum was recorded in dimethyl sulfoxide (DMSO) on a Bruker AVANCE-500 model spectrometer.

2.1.2 | Synthesis of starting materials

3-Hydroxysalicylidene-*S*-methylisothiosemicarbazone [**L_1**], was prepared by reaction of 3-hydroxysalicylaldehyde and *S*-methylisothiosemicarbazone in an equimolar ratio according to literature methods.[4,27] 4-Hydroxysalicylidene-*S*-methylisothiosemicarbazone [**L_2**] was obtained with the same method by using 4-hydroxysalicylaldehyde instead of 3-hydroxysalicylaldehyde. Characterization data of the starting materials:

[L_1]: The Color: Beige, yield 90%, m.p. (°C) 175°C-176°C. Anal. calc. $C_9H_{11}N_3O_2S$ (225 g): C, 48.00; H, 4.89; N,18.66; S, 14.22, found: C, 48.25; H, 4.82; N, 18.59; S, 14.18%. IR (cm^{-1}): ν_a(NH) 3472, ν_s(NH) 3349, ν(OH) 3218, δ(NH) 1620, ν(C = N^1), ν(N^2 = C) 1618, 1582, ν(C–O) 1162, 1139. ^{1}H-NMR: δ 11.59, 10.69 (cis/trans ratio: 5/2, s, 1H, OH), 9.05, 8.91 (cis/trans ratio: 3/7, s, 1H, R(OH)), 8.41, 8.28 (syn/anti ratio:3/7, s, 1H, CH = N^1), 6.88 (s, 2H, NH_2), 6.97-6.83 (d-d, *J* = 7.81, *J* = 1.46, 1H, *d*), 6.81-6.77 (d-d, *J* = 7.81, *J* = 1.46, 1H, *b*), 6.70 (t, 1H, *J* = 7.81, *c*), 2.44, 2.38 (cis/trans ratio:5/2, s, 3H, S-CH_3).

[L_2]: The Color: Pinkish cream, yield 92%, m.p. (°C) 179°C-180°C. Anal. calc. $C_9H_{11}N_3O_2S$ (225 g/mol): C, 48.00; H, 4.89; N,18.66; S, 14.22, found: C, 48.18; H, 4.92; N, 18.66; S, 14.27%. IR: ν_a(NH) 3445, ν_s(NH) 3337, ν(OH) 3495, δ(NH) 1624, ν(C = N^1), ν(N^2 = C) 1608, 1585, ν(C-O) 1177, 1150. NMR: 11.67, 11.02 (cis/trans ratio: 5/2, s,1H, OH), 9.75 (s, 1H, OH), 8.32, 8.20 (syn/anti ratio: 2/3, s,1H, CH = N^1), 6.71, 6.65 (syn/anti ratio: 1/1, s, 2H, NH_2), 2.42, 2.38 (cis/trans ratio: 3/2, s, 3H, S-CH_3).

2.1.3 | Synthesis of the complexes

Monochloro N(1)-3-hydroxysalicylidene-N(4)-4-methoxysalicylidene-S-methylisothiosemicarbazidato iron(III), **Fe1**: $FeCl_3.6H_2O$ (0.270 g, 1 mmol) solution in MeOH (25 mL) was added with stirring to the dissolved solution of 3-hydroxysalicylidene-*S*-methylisothiosemicarbazone (0.225 g, 1 mmol) and 4-methoxysalicylaldehyde (0.152 g, 1 mmol) in MeOH (25 mL). The black precipitate was filtered and washed with methanol-ether (1:1, 10 mL) after 2 days, and dried in vacuo over P_2O_5. The compound was crystallized in ethanol to be a single crystal.

N(1)-3-hydroxysalicylidene-N(4)-4-methoxysalicylidene-S-methylisothiosemicarbazidato nickel(II), **Ni1**, was synthesized by the reaction of 4-hydroxysalicylidene-*S*-methylisothiosemicarbazone (1 mmol) and 4-methoxysalicylaldehyde (1 mmol) by using $NiCl_2 \cdot 6H_2O$ (1 mmol) instead of $FeCl_3 \cdot 6H_2O$ with the same method.

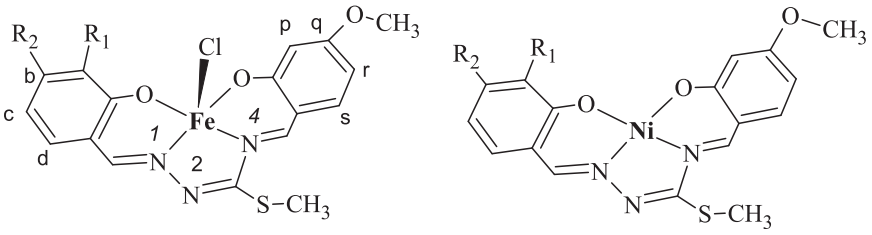

FIGURE 1 The thiosemicarbazone complexes. Arrangement of R^1/R^2 is OH/H (**Fe1**), (**Ni1**) and H/OH (**Fe2**), (**Ni2**)

TABLE 1 Crystal data and structure refinement parameters for **Fe1**

CCDC depository	1951793
Color/shape	Black/prism
Chemical formula	$[FeCl(C_{17}H_{15}N_3O_4S)] \cdot (C_2H_6O)$
Formula weight	494.75
Temperature (K)	296(2)
Wavelength (Å)	0.71073 Mo Kα
Crystal system	Triclinic
Space group	$P\bar{1}$ (No. 2)
Unit cell parameters	
a, *b*, *c* (Å)	8.0374(6), 12.7083(9), 21.9451(16)
α, *β*, *γ* (°)	102.116(6), 95.744(6), 94.008(6)
Volume (Å^3)	2171.0(3)
Z	4
$D_{calc.}$ (g/cm^3)	1.514
μ (mm^{-1})	0.949
Absorption correction	Integration
$T_{min.}$, $T_{max.}$	0.6874, 0.9589
F_{000}	1020
Crystal size (mm^3)	0.48 × 0.21 × 0.07
Diffractometer	STOE IPDS II
Measurement method	*ω* scan
Index ranges	$-10 \le h \le 10$, $-16 \le k \le 16$, $-28 \le l \le 28$
θ range for data collection (°)	$1.713 \le \theta \le 27.772$
Reflections collected	31486
Independent/observed reflections	10159/3265
$R_{int.}$	0.1481
Refinement method	Full-matrix least-squares on F^2
Data/restraints/parameters	10159/0/551
Goodness-of-fit on F^2	0.806
Final *R* indices [$I > 2\sigma(I)$]	$R_1 = 0.0587$, $wR_2 = 0.1005$
R indices (all data)	$R_1 = 0.2145$, $wR_2 = 0.1336$
$\Delta\rho_{max.}$, $\Delta\rho_{min.}$ (e/Å^3)	0.67, −0.27

Ni2 and **Fe2** complexes were obtained according to the literature.[4]

The color, yield (%), m.p. (°C), molar conductivity (ohm$^{-1} \cdot$ cm$^2 \cdot$ mol^{-1}, in 1×10^{-3} M DMSO, 25°C), $\mu_{eff.}$ (BM), elemental analysis, UV-visible (λ_{max} nm, in DMF), IR (KBr, cm^{-1}) and ^{1}H-NMR (for **Ni1** and **Ni2**) (DMSO-d$_6$, 25°C, δ ppm) data of the complexes are given as follows:

Fe1: Bright black, 24%, >399, 20.3; 5.82; Anal. calc. $C_{19}H_{21}N_3O_4SFeCl$ (448.35 g/mol-g): C, 45.50; H, 3.34; N, 9.37; S, 7.14; found: C, 45.48; H, 3.38; N, 9.40; S, 7.10%. FT-IR (KBr, cm^{-1}) *ν*(C = N) 1612, 1601, 1578, *ν*(C-O)$_{arom}$ 1158,1131, Mass: *m/z* (-c APCI): 448 (M$^+$, 100.00), 449 (MH$^+$, 21.35), 447 (M$^+$-H, 4.04), 446 (M$^+$-2H, 8.16), (+c APCI): 413 (M$^+$,-Cl, 100.00), 414 (MH$^+$,-Cl, 20.38).

Ni1: Red, 52%; 227-228; 5.6; 0.06; Anal. calc. $C_{17}H_{15}N_3O_4SNi$ (415,7 g): C, 49.07; H, 3.63; N,10.10; S, 7.71; Found: C, 49.12; H, 3.63; N, 10.05; S, 7.70%. IR (cm^{-1}): *ν*(OH) 3437, *ν*(C = N) 1609, 1597, 1580 *ν*(C-O) 1150, 1108. ^{1}H-NMR: δ 8.49 (s, 1H, O*H*), 8.19 (s, 1H, C*H* = N^1), 8.14 (s, 1H, C*H* = N^4), 6.42 (dd, *J* = 9.27, *J* = 2.44, 1H, *b*), 6.50 (t, *J* = 7.81, 1H, *c*), 7.65 (dd, *J* = 9.27, 1H, *d*), 6.47 (d, *J* = 2.44, 1H, *p*), 6.78 (dd, *J* = 7.32, *J* = 1.46, 1H, *r*), 7.01 (dd, *J* = 7.80, *J* = 1.47, 1H, *s*), 3.81 (s, 3H, O-C*H*$_3$), 2.70 (s, 3H, S-C*H*$_3$).

Fe2: Black, 19%; >390; 22.15; 5.86; Anal. calc. $C_{17}H_{15}N_3O_4SFeCl$ (448.35 g/mol-g.): C, 45.50; H, 3.34; N, 9.37; S, 7.14; Found: C, 45.48; H, 3.31; N, 9.37; S, 7.11%. IR (cm^{-1}): *ν*(OH) 3440, *ν*(C = N) 1608, 1597, 1582 *ν*(C-O) 1152, 1106. Mass: *m/z* (-c APCI): 448 (M$^+$, 100.00), 449 (MH$^+$, 22.86), 447 (M$^+$-H, 4.15), 446 (M$^+$-2H, 8.98), (+c APCI): 413 (M$^+$,-Cl, 100.00), 414 (MH$^+$,-Cl, 22.23).

Ni2: Red, 28%, 286 (decomp, °C), 8.64, 0.012. Anal. calc. $C_{17}H_{15}N_3O_4SNi$ (415.7 g mol^{-1}): C, 49.07; H, 3.63; N,10.10; S, 7.71; Found: C, 49.04; H, 3.65; N, 10.02; S, 7.67%. IR: *ν* (OH) 3437, *ν* (C = N) 1608, 1598, 1582, *ν* (C–O) 1150, 1108. ^{1}H-NMR: δ 10.08 (s, 1H, O*H*), 8.22 (s, 1H, C*H* = N^1), 8.03 (s, 1H, C*H* = N^4), 6.23 (d, *J* = 2.29, 1H, *a*), 6.21 (dd, *J* = 8.24, *J* = 2.29, 1H, *c*), 7.61 (d, *J* = 9.61, 1H, *d*), 6.46 (d, *J* = 2.29, 1H, *p*), 6.38 (dd, *J* = 9.15, *J* = 2.28, 1H, *r*), 7.34 (d, *J* = 8.69, 1H, *s*), 3.80 (s, 3H, O–C*H*$_3$), 2.66 (s, 3H, S–C*H*$_3$).

2.2 | X-ray analysis

X-ray diffraction data were recorded with an STOE IPDS II diffractometer at room temperature using graphite-monochromated Mo K*α* radiation by applying the *ω*-scan method. Data collection and cell refinement were carried out using X-AREA [28] while data reduction was applied using X-RED32.[28] The structures were solved by direct methods with SIR2019 [29] and refined by means of the full-matrix least-squares calculations on F^2 using SHELXL-2018.[30] All H atoms were placed at idealized positions and treated using a riding model, fixing the bond lengths at 0.82, 0.93, 0.97 and 0.96 Å for OH, CH, CH_2, and CH_3 atoms, respectively. The methyl and hydroxyl groups were allowed to rotate with a fixed angle around the C—X (X: C, O, and S) and C—O bonds, respectively, to best fit the experimental electron density (HFIX 137 and HFIX 147 commands of SHELXL-2018).[30] The displacement parameters of the H atoms were constrained as $U_{iso}(H) = 1.2U_{eq}$ ($1.5U_{eq}$ for OH and CH_3) of the parent atom. The crystallographic data and refinement parameters are collected in Table 1. Molecular graphics were created by using OLEX2.[31]

2.3 | Cell lines and cell culture

Caco-2 human colorectal adenocarcinoma, HCT116 human colon cancer, HT-29 human colon adenocarcinoma, HEP3B human

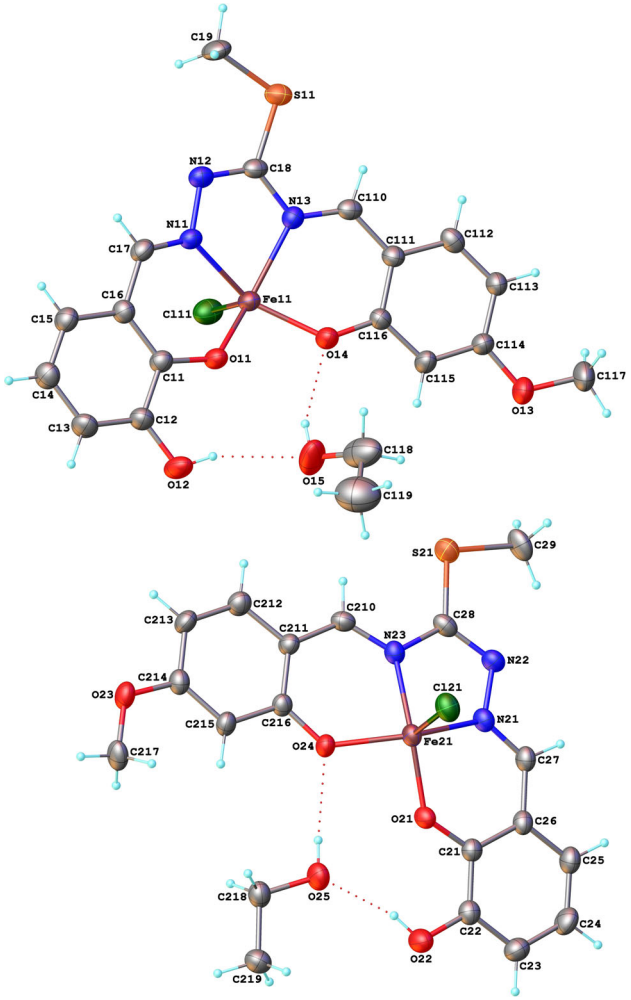

FIGURE 2 Molecular structure of **Fe1** with anisotropic displacement ellipsoids drawn at the 50% probability level

TABLE 2 Selected geometric parameters for **Fe1**

Parameters	Parameters		
Bond lengths (Å)			
Fe11—O11	1.877 (3)	Fe21—O21	1.853 (4)
Fe11—O14	1.893 (4)	Fe21—O24	1.912 (3)
Fe11—N13	2.072 (5)	Fe21—N23	2.058 (5)
Fe11—N11	2.076 (5)	Fe21—N21	2.081 (4)
Fe11—Cl11	2.208 (2)	Fe21—Cl21	2.2055 (19)
N11—C17	1.283 (6)	N21—C27	1.295 (7)
N11—N12	1.395 (6)	N21—N22	1.373 (6)
N12—C18	1.306 (6)	N22—C28	1.325 (7)
N13—C110	1.303 (6)	N23—C210	1.326 (7)
N13—C18	1.388 (7)	N23—C28	1.405 (6)
Bond angles (°)			
O11—Fe11—O14	93.51 (16)	O21—Fe21—O24	92.93 (16)
O11—Fe11—N13	143.90 (19)	O21—Fe21—N23	145.27 (17)
O14—Fe11—N13	87.77 (18)	O24—Fe21—N23	87.38 (17)
O11—Fe11—N11	86.01 (16)	O21—Fe21—N21	86.37 (17)
O14—Fe11—N11	147.1 (2)	O24—Fe21—N21	144.68 (18)
N13—Fe11—N11	74.17 (18)	N23—Fe21—N21	74.09 (19)
O11—Fe11—Cl11	109.96 (15)	O21—Fe21—Cl21	111.01 (14)
O14—Fe11—Cl11	108.77 (14)	O24—Fe21—Cl21	108.85 (12)
N13—Fe11—Cl11	103.65 (15)	N23—Fe21—Cl21	101.62 (14)
N11—Fe11—Cl11	102.24 (15)	N21—Fe21—Cl21	104.27 (14)
C17—N11—N12	114.1 (5)	C27—N21—N22	116.6 (4)
C18—N12—N11	110.6 (5)	C28—N22—N21	113.3 (4)
C110—N13—C18	121.0 (5)	C210—N23—C28	120.0 (5)
N11—C17—C16	123.3 (6)	N21—C27—C26	125.5 (5)
N12—C18—N13	120.4 (5)	N22—C28—N23	116.5 (5)
N12—C18—S11	118.6 (5)	N22—C28—S21	121.0 (4)
N13—C18—S11	121.0 (4)	N23—C28—S21	122.5 (5)
N13—C110—C111	125.9 (6)	N23—C210—C211	125.1 (5)

hepatoma, HepG2 human hepatoma cell lines were obtained from the American Type Culture Collection ATCC (VA, USA). The cells were cultured in DMEM (Dulbecco's Modified Eagle's medium; Sigma-Aldrich) supplemented with 10% fetal bovine serum (FBS; Capricorn FBS-12A), 100 units/mL penicillin and 100 μg/mL of streptomycin in a humidified incubator containing 5% CO_2 at 37°C. To reach a sufficient cell number for tests, the cells were passaged after reaching 80% monolayer confluency. Cells were sub-cultured every 2 or 3 days.

2.4 | MTT cytotoxicity assay

The MTT (3-(4,5-dimethylthiazol-2-yl)-2,5-diphenyltetrazolium bromide; Sigma-Aldrich) colorimetric assay developed by Mosmann [32] with modification was used to screen for cytotoxic activity of the compounds. Stock solutions of the compounds were prepared in DMSO (Sigma-Aldrich), and serial dilutions were made in culture medium so that the final concentration of DMSO was less than 1% (v/v) per well in all experiments. A 96-well plate was used and the assay was done in a total volume of 100 μL. Briefly, 10 μL/well of varying concentrations of thiosemicarbazone complexes (**Fe1**, **Fe2**, **Ni1**, **Ni2**) were added and subsequently the cells (90 μL/well; 10^5 cells/mL culture medium) were seeded to treat for 72 h. After the aspiration of the supernatant, and incubation with MTT solution (10 μL of 5 mg/mL PBS) at 37°C for 4 h in the dark, the cells were lysed with 100 μL dimethyl sulfoxide (DMSO). The yellow MTT dye was reduced by succinic dehydrogenase in the mitochondria of viable cells to purple formazan crystals. Absorbance was measured at 570 nm using a microplate reader.

The results were generated from three independent experiments; all experiments were performed in triplicate. The cytotoxic index was expressed as a percentage relative to the untreated control cells.

The cytotoxic concentrations of compounds that provide 50% inhibition of cell growth (IC_{50}) were calculated from the dose-response curve.

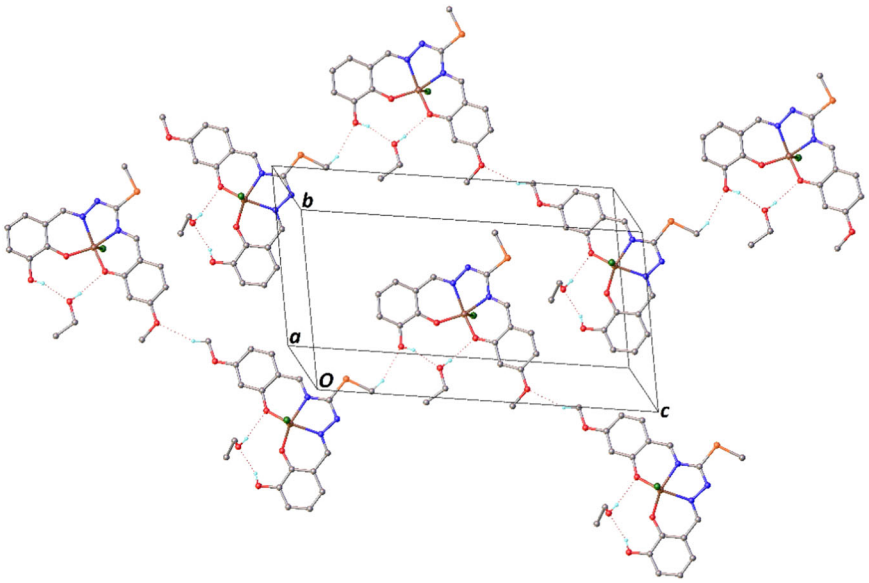

FIGURE 3 Crystal pattern of **Fe1** showing the intermolecular hydrogen bonds as dotted lines. H-atoms not involved are omitted

2.5 | Western blot immunoassay

Cell protein was extracted from lysates prepared in Cell Lysing Buffer (CLB) with freshly added PMSF(Phenylmethylsulfonyl fluoride), the protease inhibitor cocktail (1 μL) to 1 mL of extraction buffer (CLB), and kept at −20°C. All cell lysates were measured with the Bradford assay and the protein concentrations were calculated with the same method.

The proteins were separated on gels (4% stacking and 7%-10% separating gels) run at 130 V. Then the proteins were transferred to the PVDF membrane in transfer buffer at 40 mA overnight, at +4°C. Membranes were washed with Tris-buffered saline containing 1% Tween 20 (TBST), blocked for 1H in 5% non-fat milk, rinsed in TBST, and then incubated overnight at +4°C with primary antibodies. CYPs, MDR-1, MRP-1/2, and β-Actin antibodies were used at a dilution of 1:200 in 5% milk containing TBS-tween 20 buffer. After repeated washes in TBST, the membranes were incubated with horseradish peroxidase (HRP)-conjugated secondary anti-mouse or anti-goat antibody incubation with a ratio of 1:10000 in 5% milk containing TBS-tween20 for 1-hour shaking. The membranes were washed again and were visualized with ECL(Electrochemiluminescence) using a Chemiluminescence device, and pictures were taken.

TABLE 3 Hydrogen bonding geometry for **Fe1**

D—H···A	D—H (Å)	H···A (Å)	D···A (Å)	D—H···A (°)
O25—H25···O24	0.82	2.14	2.956 (6)	176
C19—H19B···O22^{i}	0.96	2.47	3.400 (7)	163
O12—H12···O15	0.82	2.20	2.990 (7)	160
O22—H22···O25	0.82	2.03	2.816 (6)	160
O15—H15···O14	0.82	2.28	3.043 (7)	155
C117—H11B···O23^{ii}	0.96	2.58	3.461 (8)	152

Symmetry codes: i: *x*, *y* + 1, *z* + 1; ii: *x* + 1, *y* + 1, *z*.

2.6 | Measurement of lipophilicity

The lipophilicity of the complexes was determined by the traditional shake-flask method [33] in *n*-octanol/PBS (pH = 7.4) buffered aqueous solution at 37°C. Ten microliters of 10 mM compounds in DMSO was mixed with an equal volume of n-octanol and PBS buffer in a test tube. The test tubes were shaken for 3 hours at 37°C and followed by standing for 15 min. After separation, 200 μL from each phase was removed and the absorptions of the solutions were measured by UV-vis (350 nm). Log *P* values were calculated according to the following equation:

$$\text{Log } P = \text{ Log } [(C_{org})/(C_{aq})],$$

C_{org}: concentrations of organic (n-octanol) phase,
C_{aq}: concentrations of aqueous (PBS) phase.

3 | RESULTS

3.1 | Chemistry

The complexes of iron(III) and nickel(II) ion, **Fe1** and **Ni1**, were synthesized by the reaction of a 3-hydroxy-salicylaldehyde-S-

TABLE 4 Cytotoxicity (as IC_{50}, μg/mL) and lipophilicity (as Log *P*) for the thiosemicarbazone complexes

Complexes	Caco-2	HCT-116	HT-29	Hep3B	HepG2	Log *P*
Fe1	0.6	0.6	1.5	0.6	1.5	0.33
Fe2	1.5	1	2.3	1.5	1.5	1.37
Ni1	>10	>10	>10	>10	>10	1.42
Ni2	>10	>10	>10	>10	>10	1.6

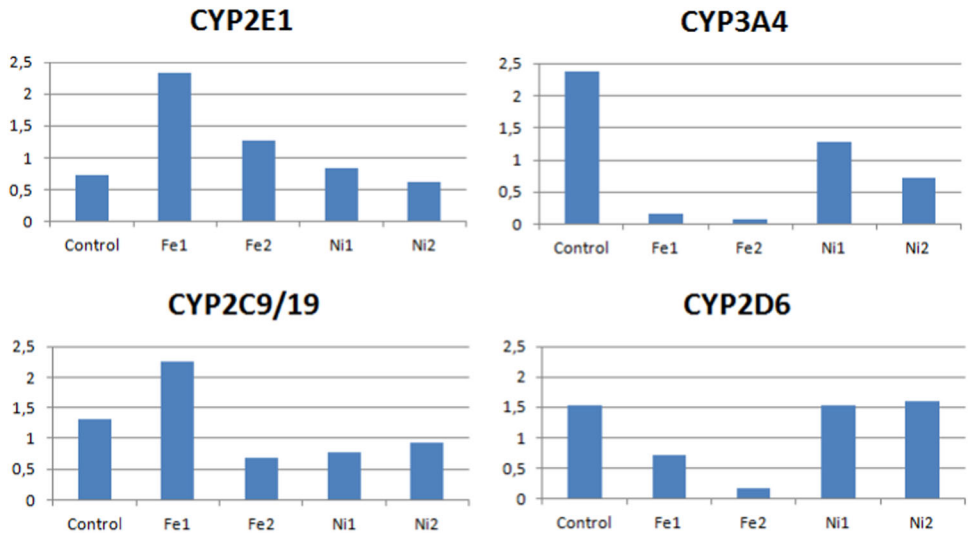

FIGURE 4 Expression levels of CYP2E1, CYP3A4, CYP2C9/19, and CYP2D6 in Caco-2 cells

methylisothiosemicarbazone and 4-methoxysalicylaldehyde in the presence of Fe(III) or Ni(II) ion. The complexes, **Fe2** and **Ni2**, were resynthesized from 4-hydroxy-salicylaldehyde-S-methylisothiosemicarbazone, 4-methoxysalicylaldehyde and the corresponding metal ion, as obtained previously.[4] The complexes were obtained as very fine powder crystals, and a single crystal of only the **Fe1** was able to be obtained in absolute ethanol for X-ray crystallography. The complexes are soluble in MeOH, EtOH and very soluble in DMF and DMSO, and are stable in air. Molar conductivity values of iron complexes, **Fe1** and **Fe2**, have high values, 20.3 and 22.15 $ohm^{-1} \cdot cm^2 \cdot mol^{-1}$, respectively, because of the chlorine atom on the iron(III) center, whereas the nickel complexes, **Ni1** and **Ni2**, have low values, 5.6 and 8.64 $ohm^{-1} \cdot cm^2 \cdot mol^{-1}$, respectively, due to non-electrolytic behaviors of the complexes.

The formation of complexes was tracked by IR spectroscopy. The stretching and bending bands attributed to the amine group of the starting material, at 3472, 3349, 1620 cm^{-1} for **[L1]**, did not appear on the IR spectra of the complexes, **Fe1** and **Ni1**. The bands attributed to (C = N) groups at 1618 and 1582 cm^{-1} for starting material **[L1]** were recorded at 1612,1601, 1578 for **Fe1**, and 1609, 1597, 1580 for **Ni1**. It was seen that a new band appeared by condensation of thioamide and the second aldehyde and the band of ($C = N^1$) was shifted to a lower wavenumber in the spectra of complexes.

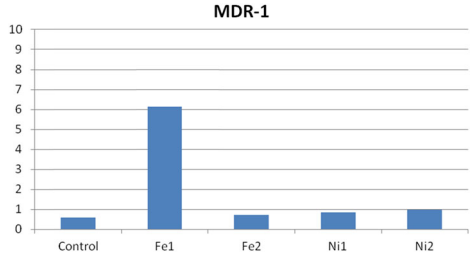

FIGURE 5 Expression levels of MDR-1 (P-gp) in Caco-2 cells

The proton signals attributed to a phenolic hydroxyl group and the amine group, at 11.59-10.69 and 6.88 ppm respectively, were not observed on the ^{1}H-NMR spectrum of the complex **Ni1**. The spectrum of **[L1]** showed the syn/anti isomerism bands at 8.41 and 8.28 ppm assigned to ($CH = N^1$). The proton signals of ($CH = N^1$) and ($CH = N^4$) groups of complex **Ni1** appeared at 8.19 and 8.14 ppm in the spectrum because of the coordination of imine groups to the nickel atom.

It was reported by IR and ^{1}H-NMR spectra that the chelate formed from the starting material and 4-methoxysalicylaldehyde was coordinated to the nickel ion through imine and phenolic hydroxyl groups.

3.2 | Single-crystal structure determination

The molecular diagram of **Fe1** with the adopted atom-labeling scheme is shown in Figure 2, while important bond lengths and angles are listed in Table 2. There are two crystallographically independent but chemically equal complex molecules A and B as well as two ethanol solvent molecules per asymmetric unit. Atoms are labeled 1nn for A and 2nn for B. The molecular structures are almost superimposable except for the methoxy groups as shown in Figure 2. In the following discussion, parameters for B are given in square brackets, see also Table 2.

The compound $FeCl(C_{17}H_{15}N_3O_4S) \cdot C_2H_6O$ (**Fe1**) shows a Fe(III) center coordinated with a methyl (*E*)-*N*′-[(*E*)-2, 3-dihydroxybenzylidene]-*N*-[(E)-2-hydroxy-4-methoxybenzylidene] carbamohydrazonothioate ligand and one Cl ligand to reach a slightly distorted square-pyramidal coordination with two phenolate oxygens and two azomethine nitrogens and the apical Cl. The coordination geometry is also supported by the τ_5 parameter [34] of 0.05 [0.01]. The Fe—N, Fe—O, and Fe—Cl bond lengths are 2.072(5) and 2.076(5) Å [2.058(5) and 2.081(4) Å], 1.877(3) and 1.893(4) Å [1.853(4) and

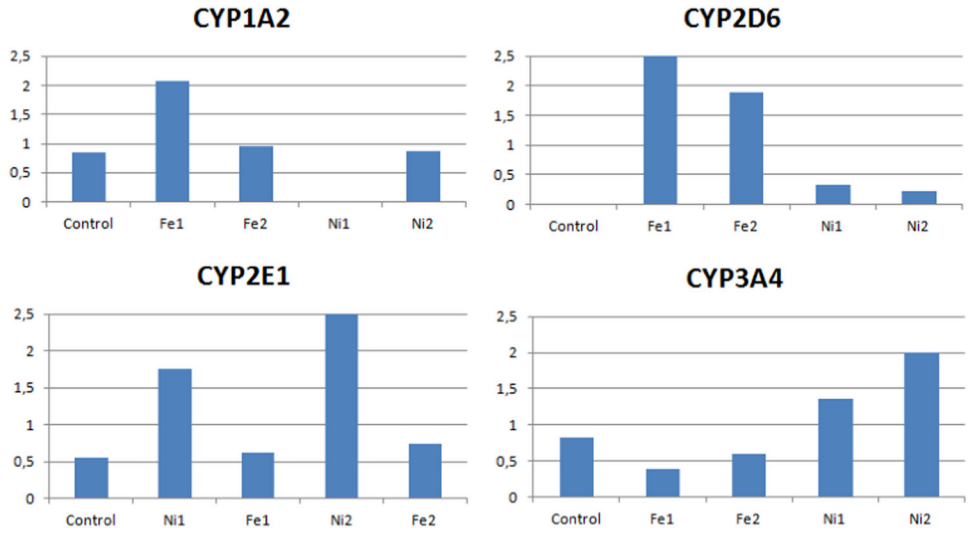

FIGURE 6 Expression levels of CYP1A2, CYP2D6, CYP2E1, and CYP3A4 in HCT-116 cells

1.912(3) Å], and 2.208(2) Å [2.2055(19) Å], respectively, which agree well with those known from literature.[4,35–39] The Fe atom is situated 0.5573(9) Å [0.5665(8) Å] above the N_2O_2 plane towards the Cl ligand. This is also reflected by the O—Fe—N trans angles of 143.90(19) and 147.1(2)° [145.27(17) and 144.68(18)°]. There is one five-membered FeN_3C and two six-membered $FeNC_3O$ chelate rings.

In the crystal structure, intermolecular hydrogen bonds O12—H12···O15, O15—H15···O14, O22—H22···O25, and O25—H25···O24 link the solvent and complex molecules to each other, as shown in Figure 2. Additional C19—H19B···O22 (x, $y+1$, $z+1$) and C117—H11B···O23 ($x+1$, $y+1$, z) interactions are observed that stabilize the packing (Figure 3). The full information is given in Table 3. There are no intramolecular hydrogen bonds shorter than the van-der-Waals contacts.

3.3 | Cytotoxicity of thiosemicarbazone complexes against cancer cell lines

The cytotoxic concentrations of thiosemicarbazone derivatives that provide 50% inhibition of cell growth (IC_{50}) are shown in Table 4. The lowest IC_{50} value shows a better cytotoxic effect. Microscopic images of HepG2 cells were chosen as a representative demonstration (Figure 13).

3.4 | Lipophilicity (Log *P*) of thiosemicarbazone complexes

LogP (lipophilicity) was defined and calculated as the logarithm of the ratio of the concentrations of the complexes in the organic and aqueous phases (Table 4).

As seen in Table 4, Log *P* values can range from **Fe1** < **Fe2** < **Ni1** < **Ni2**.

3.5 | CYPs, P-gp (MDR-1) and MRP-1 protein expression levels undertaken by Western blot immunoassay

Five Cytochrome P450 (CYP) enzymes (CYP3A4, CYP1A2, CYP2D6, CYP2E1, CYP2C9/19), P-glycoprotein (MDR-1) and MRP-1 protein expressions were detected. Colon and hepatocyte cell lines were treated with IC_{50} values of the

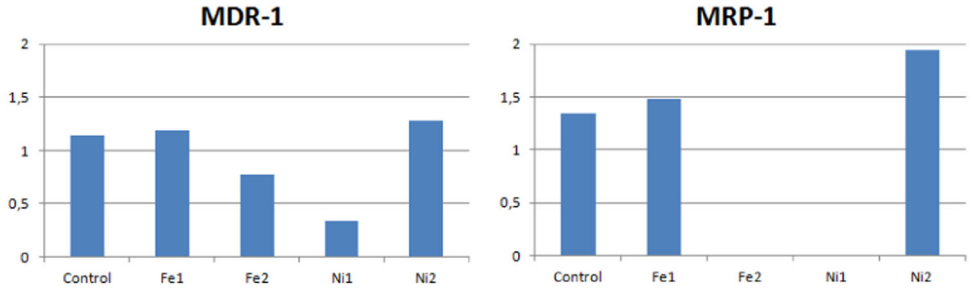

FIGURE 7 Expression levels of MDR-1 (P-gp) and MRP-1 in HCT-116 cells

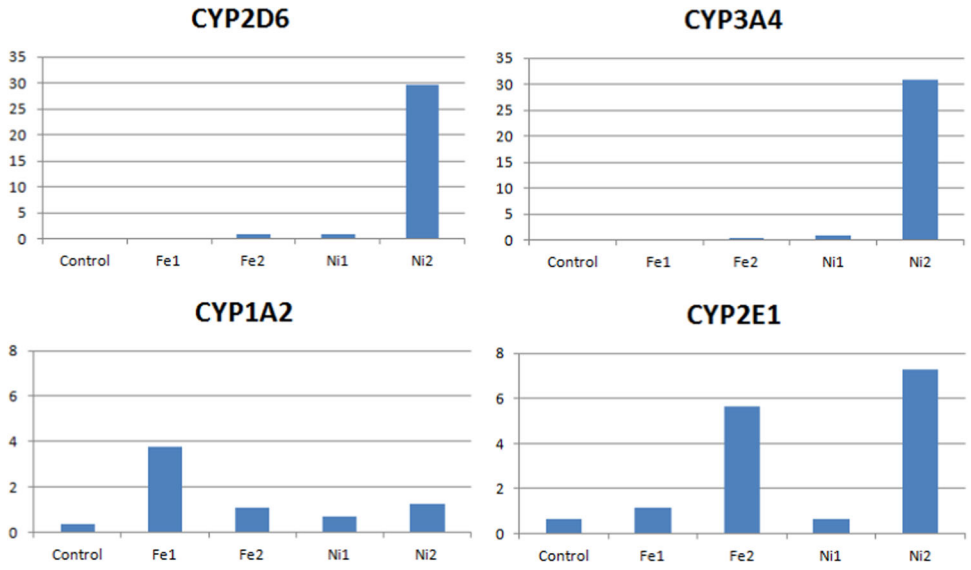

FIGURE 8 Expression levels of CYP2D6, CYP3A4, CYP1A2, and CYP2E1 in HT-29 cells

thiosemicarbazone complexes (**Fe1**, **Fe2**, **Ni1**, **Ni2**), and untreated cells were used as controls. β-Actin was the loading control for the Western blot and used for calculating protein expression levels. Band intensities (*y* axis) quantified by ImageJ software (Figures 4-12).

The results of Western blot studies indicate that each compound is metabolized by different enzymes in each cell line. Also, HCT116 cells used in experiments are resistant (P-gp positive) to the chemotherapeutics.

4 | DISCUSSION

Fe(III) and Ni(II) complexes were synthesized by the reaction of R-substitute-salicylaldehyde-*S*-methylisothiosemicarbazone (R:3-OH, 4-OH) and 4-methoxysalicylaldehyde. The X-ray study shows that the ligand behaves as a dinegative tetradentate N_2O_2 chelate in the presence of metal ions. The occupation of the apical position by a chloride atom results in a distorted square-pyramidal geometry. The determination of the pharmacokinetic properties of the newly synthesized thiosemicarbazone derivatives is important in that they can be used as potential anticancer agents. Cytotoxic activities of some thiosemicarbazones previously synthesized by Ülküseven and his coworkers have been investigated with the potential to become anticancer drugs with a series of studies on the K562 leukemia cell line.[4,27,40] Among these compounds, two of the most effective (**Fe2** and **Ni2**) and two new compounds (**Fe1**, **Ni1**) were selected and primarily IC_{50} values were found in vitro hepatocyte (Hep3B and HepG2) and colon (Caco-2, HCT-116, and HT-29) cell lines. The lowest inhibitory concentration (0.6 μg/mL in Caco-2, HCT-116, Hep3B and 1.5 μg/mL in HepG2 and HT-29) determined by the MTT cytotoxicity method was detected in cell lines treated with **Fe1**. In cells treated with **Fe2**, the IC_{50} values were 1.5 μg/mL for Caco-2, HepG2, and Hep3B; 1 μg/mL for HCT-116; and 2.3 μg/mL for HT-29. In the nickel complexes, the IC_{50} was >10 μg/mL.

Another parameter that is used to determine the pharmacokinetic properties of the potential medicinally investigated substances is lipophilicity. In this study, the most common and easily applied method, the shake-flask method, was used to find lipophilicity values. Akgemci et al[41] found the LogP values of their synthesized thiosemicarbazone compounds to be 1.15 and 1.95, by using this method.[41] In oral administration of drugs, the lipophilicity is required to be $0 \leq \text{Log } P \leq 3$.[42] In this paper, lipophilicity (Log *P*) values were calculated in the range of 0.33-1.6 and was observed decreasing in Log *P* in the order of **Fe1** < **Fe2** < **Ni1** < **Ni2.** The lipophilicity of the thiosemicarbazone complexes in this study was found to be in the range of desirable values. Also, there is a relationship between the IC_{50} values determined by the MTT assay and the lipophilicity (Log *P*) values. Accordingly, the lower LogP value is also low for the lower IC_{50} value. Furthermore, Fe-containing compounds have lower LogP values. Therefore, the solubility of the iron-containing compounds is better than those containing nickel. Thus, Fe-containing compounds have been effective even in very low concentrations as their entry into the cell is easier.

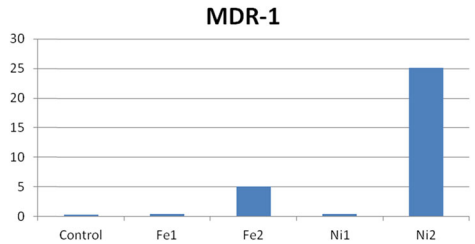

FIGURE 9 Expression levels of MDR-1 (P-gp) in HT-29 cells

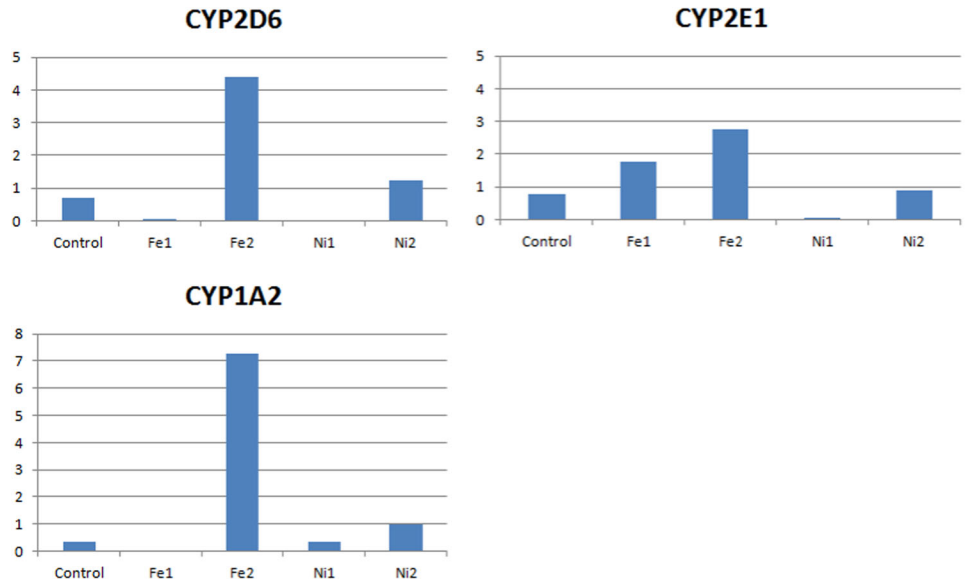

FIGURE 10 Expression levels of CYP2D6, CYP2E1, and CYP1A2 in Hep3B cells

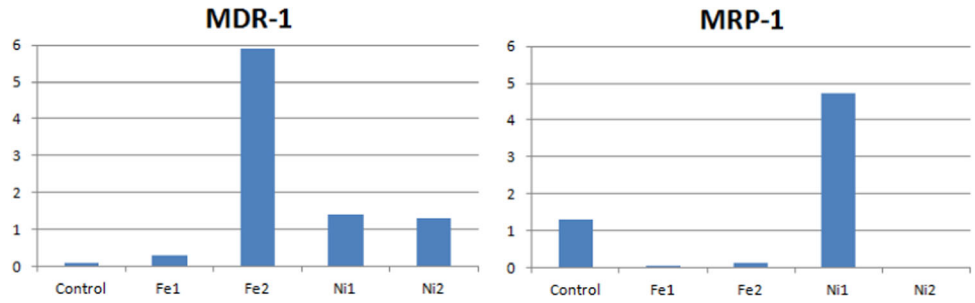

FIGURE 11 Expression levels of MDR-1 (P-gl) and MRP-1 in Hep3B cells

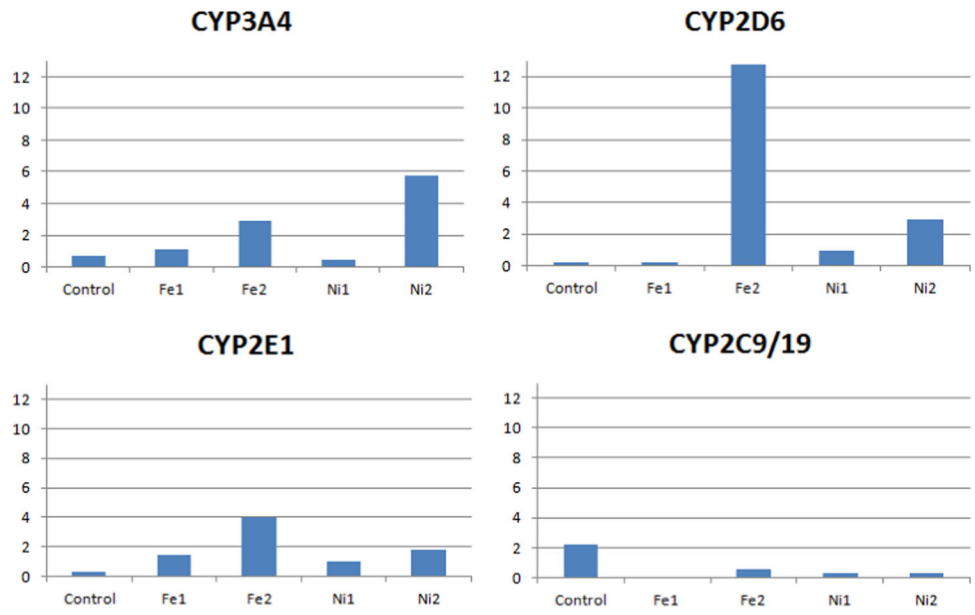

FIGURE 12 Expression levels of CYP3A4, CYP2D6, CYP2E1, and CYP2C9/19 in HepG2 cells

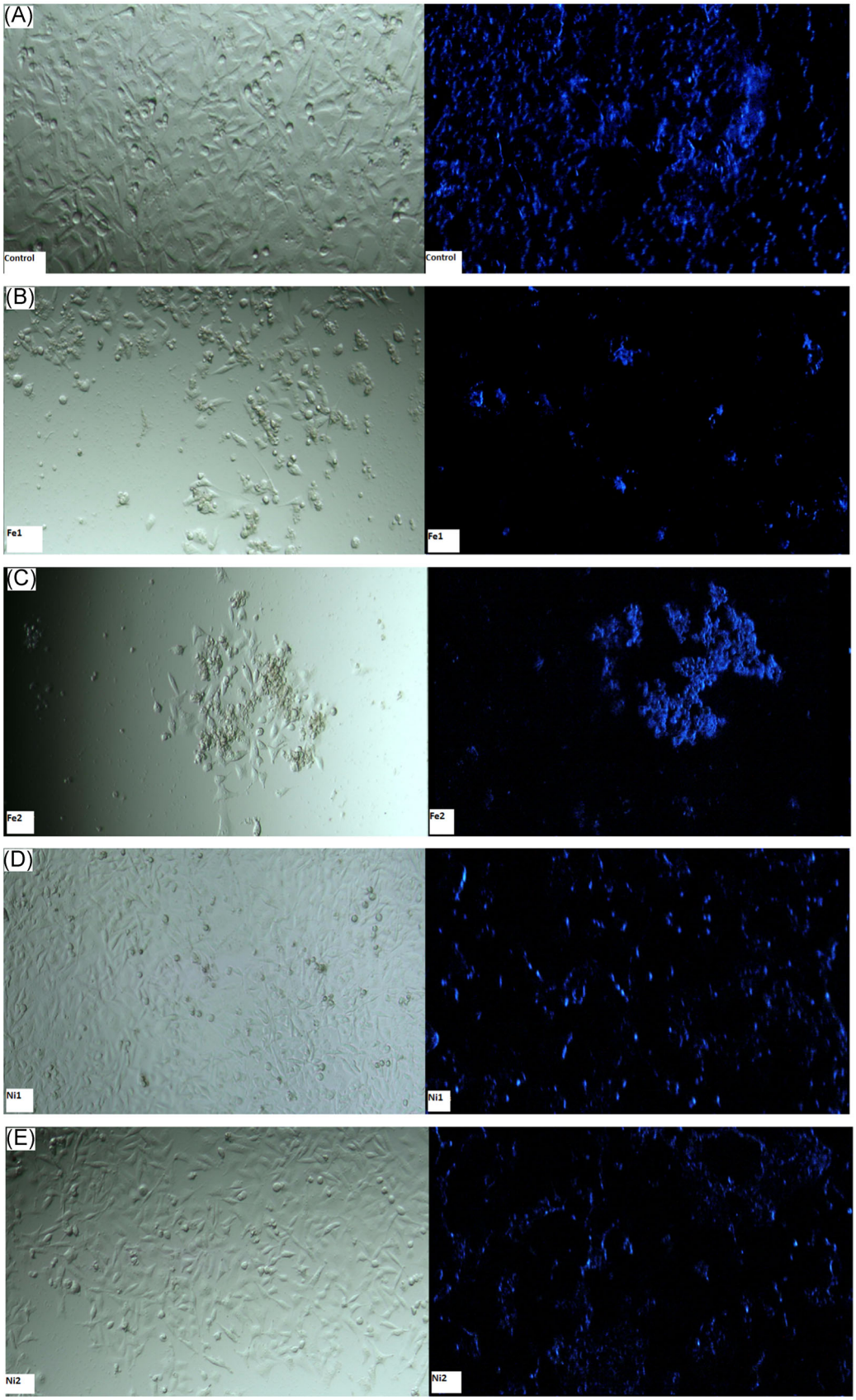

FIGURE 13 Inverted (left column) and fluorescence (right column) microscopy images of HepG2 cells untreated (control) (A) and treated with complexes Fe1, Fe2, Ni1, and Ni2 (B,C,D,E) in IC_{50} concentrations. Cells were stained with DAPI (blue); IC_{50}, 50% inhibition of cell growth

TABLE 5 Expression levels of CYP enzymes according to the cells and the complexes (↑increase, ↓decrease, n/a: not available)

Cell lines/ Enzymes	Caco-2	HCT-116	HT-29	Hep3B	HepG2
CYP3A4	Fe1 ↓ Fe2	Fe1 ↓ Ni1 ↑ Fe2 Ni2	Ni2 ↑	n/a	Ni2 ↑ Fe2
CYP2D6	Fe1 ↓ Fe2	Fe1 ↑ Fe2	Ni2 ↑	Fe2 ↑	n/a
CYP2E1	Fe1 ↑ Fe2	Ni1, Fe1 ↑ Ni2, Fe2	Ni2 ↑ Fe2	Fe1 ↑ Fe2	Ni1, Fe1 ↑ Ni2, Fe2
CYP1A2	n/a	Fe1 ↑ Fe2	Fe1 ↑	Fe2 ↑	n/a
CYP2C9/19	Fe1 ↑	n/a	n/a	n/a	Ni1, Fe1 ↓ Ni2, Fe2
MDR-1	Fe1 ↑	Ni1 ↓ Control ↑ Fe2 Fe1,Ni2	Ni2 ↑ Fe2	Fe2 ↑	
MRP-1		Ni1 ↓ Control ↑ Fe2 Fe1,Ni2		Ni1 ↑	

P-glycoprotein (MDR-1), which is located in the cell membrane and pumps drugs out of the cell and five enzymes (CYP3A4, CYP2E1, CYP2C9/19, CYP2E1, CYP2D6) belonging to the cytochrome P450 (CYP) family metabolizing drugs from ADMET reactions, and MRP-1 (multidrug resistance protein) were examined by Western blot. According to the obtained data, each substance is metabolized by different enzymes in each cell line. Although HCT-116 colon cancer cells were spontaneously found to be P-gp positive, the Fe-containing thiosemicarbazones used in the experiments were found to be effective by breaking this resistance.

Besides this, in the biotransformation of other drugs, a compound can be metabolized by more than one enzyme.[43] In tamoxifen, used in breast cancer treatment, the biotransformation process is performed with both the CYP2D6 enzyme (4-hydroxylation) and CYP3A4/5 enzyme (N-demethylation).[43] An in vitro study about thiosemicarbazone derivatives showing anti-trypanosomatids activity demonstrated a safe toxicological profile against four human cell lines (A549-lung adenocarcinoma, W1-38-caucasian fibroblast-like fetal lung, THP-1-derived macrophages, U2OS-osteosarcoma cells) with a panel of five cytochrome p450 isoforms (1A2, 2C9, 2C19, 2D6, 3A4).[44] There is only one in vivo study in the literature about the metabolism of thiosemicarbazones. In this in vivo study, thiosemicarbazone derivatives used as anticonvulsants have modestly activated CYP2C9 and CYP2D6 enzymes inhibited CYP1A2 enzyme and found no change in the activity of CYP2A6, CYP2B6, CYP2C19, CYP2E1, and CYP3A4 enzymes.[45]

In our study, it was observed that the compounds had a safe toxicological profile similar to the above studies. As seen from

Table 5, the protein expression levels of CYP3A4 decrease in colon (HCT-116, Caco-2) cell lines with exposure of Fe-containing (**Fe1**, **Fe2**) compounds. Treatment with **Fe1** and **Fe2** compounds cause decrease of CYP2D6 in Caco-2 cells and increases the expression levels of CYP2D6 and CYP1A2 in the HCT-116 cells. Generally, the expression levels of CYP2E1 increase in all cell lines in all compounds exposure. Expression levels of CYP1A2 increase in HCT-116, HT-29 and Hep3B with Fe-containing (**Fe1**, **Fe2**) compounds treatment. In HepG2 cells, the expression levels of CYP2C9/19 decrease with all four compounds' exposure.

In other words, **Ni1** is metabolized by CYP3A4 and CYP2E1 in HCT-116 and HepG2 cell lines. **Fe1** is metabolized by CYP2D6, CYP2E1, CYP1A2, and CYP2C9/19 in all cell lines. **Ni2** is metabolized by CYP3A4, CYP2D6 and CYP2E1 in HCT-116, HT-29, HepG2 cell lines. **Fe2** is metabolized by CYP3A4, CYP2D6, CYP2E1, CYP1A2 in all cell lines. Remarkably, Fe-containing compounds (**Fe1**, **Fe2**) have a lower IC_{50} value and are metabolized in all cell lines.

5 | CONCLUSIONS

In conclusion, in this study, several parameters that may influence the pharmacokinetic properties of thiosemicarbazone compounds, which are potential new synthesized anticancer drugs, have been investigated in vitro. Considering all the data, four thiosemicarbazone derivatives are metabolized by at least one CYP enzyme in both colon and hepatic cell lines. A correlation was found between IC_{50} values and lipophilicity. The X-ray study shows that the thiosemicarbazone ligand behaves as a dinegative tetradentate N_2O_2 chelate in the presence of the metal ion. Occupation of the fifth coordination by a chloride atom results in a distorted square-pyramidal geometry.

In this present study, the pharmacokinetic properties of newly synthesized thiosemicarbazone compounds as oral medicaments were investigated in vitro and obtained information that could be a source for future in vivo investigations.

ACKNOWLEDGMENTS

This study was supported by the Scientific Research Projects Coordination Unit of Istanbul University (Project number: 49111); the Ondokuz Mayıs University (Project No: PYO.FEN.1906.19.001); and TÜBİTAK-SBAG (Project Number: 109S188).

CONFLICT OF INTERESTS

The authors declare that there are no conflict of interests.

ORCID

Mediha Süleymanoğlu http://orcid.org/0000-0002-1401-4863
Serap Erdem-Kuruca http://orcid.org/0000-0001-7878-9994
Tülay Bal-Demirci http://orcid.org/0000-0003-4663-2209
Namık Özdemir http://orcid.org/0000-0003-3371-9874
Bahri Ülküseven http://orcid.org/0000-0001-6342-1505
İlhan Yaylım http://orcid.org/0000-0003-2615-0202

REFERENCES

[1] D. X. West, S. B. Padhye, P. B. Sonawane, *Complex Chemistry*, Structural and physical correlations in the biological properties of transition metal heterocyclic thiosemicarbazone and S-alkyldithiocarbazate complexes, Springer, Berlin, Heidelberg **1991**, pp. 1–50. https://doi.org/10.1007/3-540-53499-7_1
[2] D. X. West, A. E. Liberta, S. B. Padhye, R. C. Chikate, P. B. Sonawane, A. S. Kumbhar, R. G. Yerande, *Coord. Chem. Rev.* **1993**, *123*, 49. https://doi.org/10.1016/0010-8545(93)85052-6
[3] S. Padhye, G. B. Kauffman, *Coord. Chem. Rev.* **1985**, *63*, 127. https://doi.org/10.1016/0010-8545(85)80022-9
[4] T. Bal-Demirci, G. Congur, A. Erdem, S. Erdem-Kuruca, N. Özdemir, K. Akgün-Dar, B. Varol, B. Ülküseven, *New J. Chem.* **2015**, *39*, 5643. https://doi.org/10.1039/C5NJ00594A
[5] E. Avcu Altiparmak, G. Ozen Eroglu, E. Ozcelik, N. Özdemir, S. Erdem Kuruca, N. Arsu, B. Ülküseven, T. Bal-Demirci, *Appl. Organomet. Chem.* **2019**, *33*, e5023. https://doi.org/10.1002/aoc.5023
[6] I. Haiduc, C. Silvestru, *Coord. Chem. Rev.* **1990**, *99*, 253. https://doi.org/10.1016/0010-8545(90)80065-2
[7] T. Bal, B. Ülküseven, *Russ. J. Inorg. Chem.* **2004**, *49*, 1685. https://doi.org/10.1007/s11243-004-2240-y
[8] P. Kalaivani, R. Prabhakaran, E. Ramachandran, F. Dallemer, G. Paramaguru, R. Renganathan, P. Poornima, V. V. Padma, K. Natarajan, *Dalton Trans.* **2012**, *41*, 2486. https://doi.org/10.1039/C1DT11838B
[9] S. A. Khan, M. Yusuf, *Eur. J. Med. Chem.* **2009**, *44*, 2270. https://doi.org/10.1016/j.ejmech.2008.06.008
[10] P. W. Sadler, *Journal of the Chemical Society Resumed* **1961**, 243. https://doi.org/10.1039/JR9610000243
[11] J. Lowe, *Lancet* **1954**, *264*, 1065. https://doi.org/10.1016/S0140-6736(54)90622-4
[12] E. M. Bavin, R. J. Rees, J. M. Robson, M. Seiler, D. E. Seymour, D. Suddaby, *J. Pharm. Pharmacol.* **1950**, *2*, 764. https://doi.org/10.1111/j.2042-7158.1950.tb12999.x
[13] R. B. de Oliveira, E. M. de Souza-Fagundes, R. P. Soares, A. A. Andrade, A. U. Krettli, C. L. Zani, *Eur. J. Med. Chem.* **2008**, *43*, 1983. https://doi.org/10.1016/j.ejmech.2007.11.012
[14] C. M. Nutting, C. M. Van Herpen, A. B. Miah, S. A. Bhide, J. P. Machiels, J. Buter, C. Kelly, D. De Raucourt, K. J. Harrington, *Ann. Oncol.* **2009**, *20*, 1275. https://doi.org/10.1093/annonc/mdn775
[15] K. Y. Salim, S. M. Vareki, W. R. Danter, J. Koropatnick, *Oncotarget* **2016**, *7*, 41363. https://doi.org/10.18632/oncotarget.9133
[16] A. Lindemann, A. A. Patel, N. L. Silver, L. Tang, Z. Liu, L. Wang, N. Tanaka, X. Rao, H. Takahashi, N. K. Maduka, M. Zhao, *Clin. Cancer Res.* **2019**, *25*, 5650. https://doi.org/10.1158/1078-0432.CCR-19-0096
[17] L. C. Dias, G. M. de Lima, C. B. Pinheiro, M. A. Nascimento, R. S. Bitzer, *J. Mol. Struct.* **2017**, *1131*, 79. https://doi.org/10.1016/j.molstruc.2016.11.039
[18] J. Lowe, *Lancet* **1952**, *259*, 436. https://doi.org/10.1016/s0140-6736(52)91951-x
[19] C. A. Kunos, T. Radivoyevitch, S. Waggoner, R. Debernardo, K. Zanotti, K. Resnick, N. Fusco, R. Adams, R. Redline, P. Faulhaber, A. Dowlati, *Gynecol. Oncol.* **2013**, *130*, 75. https://doi.org/10.1016/j.ygyno.2013.04.019
[20] M. Serda, A. Mrozek-Wilczkiewicz, J. Jampilek, M. Pesko, K. Kralova, M. Vejsova, R. Musiol, A. Ratuszna, J. Polanski, *Molecules* **2012**, *17*, 13483. https://doi.org/10.3390/molecules171113483
[21] E. Anzenbacherová, J. Janalík, I. Popa, M. Strnad, P. Anzenbacher, *Biomedical Papers-Palacky University in Olomouc* **2005**, *149*, 349. https://doi.org/10.5507/bp.2005.056
[22] N. Kanayama, C. Kanari, Y. Masuda, S. Ohmori, T. Ooie, *Xenobiotica* **2007**, *37*, 139. https://doi.org/10.1080/00498250601140072
[23] H. Glaeser, D. G. Bailey, G. K. Dresser, J. C. Gregor, U. I. Schwarz, J. S. McGrath, E. Jolicoeur, W. Lee, B. F. Leake, R. G. Tirona, R. B. Kim, *Clinical Pharmacology & Therapeutics* **2007**, *81*, 362. https://doi.org/10.1038/sj.clpt.6100056

[24] R. D. Bruno, V. C. Njar, *Bioorg. Med. Chem.* **2007**, *15*, 5047. https://doi.org/10.1016/j.bmc.2007.05.046
[25] B. D. Tülay, U. Bahri, K. D. Serap. New thiosemicarbazone chelates having anticancer activity. **2018**. EP2881399 (A1); EP2881399 (B1).
[26] U. Bahri, B. D. Tülay, K. D. Serap. Antikanser Aktiviteye Sahip Yeni Tiyosemikarbazon Şelatları. **2019**. TR201819166T4.
[27] B. Atasever, B. Ülküseven, T. Bal-Demirci, S. Erdem-Kuruca, Z. Solakoğlu, *Invest. New Drugs* **2010**, *28*, 421. https://doi.org/10.1007/s10637-009-9272-2
[28] C. Stoe, *X-AREA Version118 and X-RED Version104*, Stoe & Cie, Darmstadt, Germany **2002**.
[29] M. C. Burla, R. Caliandro, B. Carrozzini, G. L. Cascarano, C. Cuocci, C. Giacovazzo, M. Mallamo, A. Mazzone, G. Polidori, *J. Appl. Crystallogr.* **2015**, *48*, 306. https://doi.org/10.1107/S1600576715001132
[30] G. M. Sheldrick, *Acta Crystallogr. Sect. A: Found. Adv.* **2015**, *71*, 3. https://doi.org/10.1107/S2053273314026370
[31] O. V. Dolomanov, L. J. Bourhis, R. J. Gildea, J. A. Howard, H. Puschmann, *J. Appl. Crystallogr.* **2009**, *42*, 339. https://doi.org/10.1107/S0021889808042726
[32] T. Mosmann, *J. Immunol. Methods* **1983**, *65*, 55. https://doi.org/10.1016/0022-1759(83)90303-4
[33] S. Kadowaki, M. Munekane, Y. Kitamura, M. Hiromura, S. Kamino, Y. Yoshikawa, H. Saji, S. Enomoto, *Biol. Trace Elem. Res.* **2013**, *154*, 111. https://doi.org/10.1007/s12011-013-9704-x
[34] A. W. Addison, T. N. Rao, J. Reedijk, J. van Rijn, G. C. Synthesis Verschoor, *J. Chem. Soc. Dalton Trans.* **1984**, *7*, 1349. https://doi.org/10.1039/DT9840001349
[35] M. Ahmadi, J. T. Mague, A. Akbari, R. Takjoo, *Polyhedron* **2012**, *42*, 128. https://doi.org/10.1016/j.poly.2012.05.004
[36] Y. D. Kurt, B. Ülküseven, S. Tuna, M. Ergüven, S. Solakoğlu, *J. Coord. Chem.* **2009**, *62*, 2172. https://doi.org/10.1080/00958970902787775
[37] B. Kaya, O. Şahin, M. Bener, B. Ülküseven, *J. Mol. Struct.* **2018**, *1167*, 16. https://doi.org/10.1016/j.molstruc.2018.04.082
[38] Y. Kurt, N. G. Deniz, *J. Coord. Chem.* **2015**, *68*, 4070. https://doi.org/10.1080/00958972.2015.1086760
[39] R. Takjoo, J. T. Mague, A. Akbari, M. Ahmadi, *J. Coord. Chem.* **2013**, *66*, 3915. https://doi.org/10.1080/00958972.2013.856420
[40] T. Bal, B. Atasever, Z. Solakoğlu, S. Erdem-Kuruca, B. Ülküseven, *Eur. J. Med. Chem.* **2007**, *42*, 161. https://doi.org/10.1016/j.ejmech.2006.09.004
[41] E. G. Akgemci, H. Bingol, M. Ozcelik, M. Ersoz, *Acta Phys.-Chim. Sin.* **2008**, *24*, 619. https://doi.org/10.1016/S1872-1508(08)60028-5
[42] L. Di, E. H. Kerns, *Drug-like Properties: Concepts, Structure Design and Methods from ADME to Toxicity Optimization*, Academic Press, **2015**, https://doi.org/10.1016/b978-012369520-8.50024-3
[43] K. I. Fujita, *Curr. Drug Metab.* **2006**, *7*, 23. https://doi.org/10.2174/138920006774832587
[44] P. Linciano, C. B. Moraes, L. M. Alcantara, C. H. Franco, B. Pascoalino, L. H. Freitas-Junior, S. Macedo, N. Santarem, A. Cordeiro-da-Silva, S. Gul, G. Witt, *Eur. J. Med. Chem.* **2018**, *146*, 423. https://doi.org/10.1016/j.ejmech.2018.01.043
[45] P. Singh, J. Jain, R. Sinha, A. Samad, R. Kumar, M. Malhotra, *Central Nervous System Agents in Medicinal Chemistry Formerly Current Medicinal Chemistry Central Nervous System Agents* **2011**, *11*, 60. https://doi.org/10.2174/187152411794961112

SUPPORTING INFORMATION

Additional supporting information may be found online in the Supporting Information section.

How to cite this article: Süleymanoğlu M, Erdem-Kuruca S, Bal-Demirci T, Özdemir N, Ülküseven B, Yaylım İ. Synthesis, structural, cytotoxic and pharmacokinetic evaluation of some thiosemicarbazone derivatives. *J Biochem Mol Toxicol*. 2020;e22512. https://doi.org/10.1002/jbt.22512